Larhyss Journal, ISSN 1112-3680, n°59, Sept 2024, pp157-179

A NEW TRAPEZOIDAL FLUME FOR OPEN CHANNEL FLOW MEASUREMENT DESIGN, THEORY, AND EXPERIMENT

ACHOUR B.[1*], MEHTA D.[2], AZAMATHULLA H.M.[3]

[1] Professor, Research Laboratory in Subterranean and Surface Hydraulics (LARHYSS), University of Biskra, Algeria
[2] Assistant Professor, Department of Civil Engineering, Dr. S. & S. S. Ghandhy Government Engineering College, Surat, Gujarat, India
[3] Professor, Department of Civil & Environmental Engineering, The University of the West Indies, St. Augustine Campus, Trinidad

(*) bachir.achour@larhyss.net

Research Article – Available at http://larhyss.net/ojs/index.php/larhyss/index
Received April 2, 2024, Received in revised form August 28, 2024, Accepted September 1, 2024

ABSTRACT

Several means are used for flow measurement, including the flumes that are of interest to the present study. The operating principle of the flume is based on the lateral contraction of the walls of a trapezoidal channel that ends in a triangular section extended by a throat of the same section. The convergent part of the flume accelerates the flow from a subcritical state to a critical state in the throat where a control section is created. Thus, the flow can be determined by taking a single depth reading in the inlet cross-section of the flume.

The recommended device is simple and compact in shape, requiring a minimum of space compared to known trapezoidal flumes. Furthermore, the device has been designed to be used in open channels regardless of the shape. Therefore, the flume has the property of being of a universal range.

A rigorous theoretical development led to the derivation of the governing discharge coefficient C_d relationship, solely depending on the dimensionless parameter $M_1 = mh_1/b_1$, where m is the side slope of the flume, h_1 is the upstream flow depth, and b_1 is the inlet cross-section width of the converging part of the flume.

Based on 1023 pairs of values Q-h_1 collected from twelve tested flumes of different practical dimensions, the in-depth analysis of laboratory observations corroborated the validity and reliability of the theoretical relationship governing C_d within the wide range $0.10 \leq M_1 \leq 0.95$, since the maximum deviation is only 0.215% when compared to observations.

Among the twelve tested devices, only the results of the observations carried out on one device will be presented herein. The observations collected on this device are considered the most unfavourable compared with those carried out on the eleven other tested devices, especially regarding the deviation affecting the discharge coefficient C_d.

Keywords: Trapezoidal flume, Discharge coefficient, Discharge, Stage-discharge relationship, Flow measurement

INTRODUCTION

Flow measurement has become essential in the field of water and, in particular, the sanitation of urban and industrial water. The installation of flow measurement equipment often responds to a water agency request but will also serve to provide a better understanding of the operation of the structures. Flow measurement has been practiced for a very long time. The fountain engineers, sometimes called fountain workers, and builders of aqueducts of yesteryear had to know the water flow rates to size their canals and control them. At that time, gauges with holes were used. The measurement did not take into account the flow velocity, and this is how this method was called the "direct discharge method" (Bos, 1989; Achour et al., 2003; Achour et al., 2022a; Achour et al., 2022b), which is still the most preferred method today, including the flumes that interest our study. The direct discharge method uses devices for the direct measurement of the flow rate sought through a relationship, often empirical, called the stage-discharge relationship. By introducing the measured upstream depth into this relationship, the corresponding flow rate Q is determined, provided that the dimensions of the device are given. In this case, the device is defined as semi-modular, unlike modular devices whose flow rate depends only on its geometric characteristics, such as siphons sized for a given flow rate, or Neyrpic's modular mask (Carlier, 1987; Achour, 1989).

Such as weirs which are often used to measure flow rate in open channels, and are well described in the following relevant references (Gouryev et al., 2020; Kulkarni and Hinge, 2021; Achour and Amara, 2021a; Achour and Amara, 2021b; Amara and Achour, 2021; Achour and Amara, 2022c; Achour et al., 2022d; Achour and Amara, 2022f; Kulkarni and Hinge, 2023; Achour and Amara, 2023), flumes are also well detailed in the following specialized literature (Hager, 1986; Bos, 1989), and are the most commonly used structures, such as: Achour's hydraulic jump flowmeter (1989); Achour and De Lapray flowmeter (2023), whose walls are curved forming a convergent triangular channel; Replogle-Bos-Clemens (RBC) flumes (Replogle, 1975), which are fully portable flumes for a canal or water channel comprising a horizontal sill across the width device; cutthroat flumes initiated by Skogerboe et al. (Skogerboe et al., 1972), which are devoid of a throat, hence the name "Cutthroat", unlike many other flumes and are simply formed by converging and diverging sections; SM-Flume (Samani and Magallanez, 2000); circular flumes (Samani et al., 1991); central baffle flumes, whose theoretical flow rate relationship was derived using dimensional analysis (Ferro, 2016); and the calibration of the derived relationship was carried out with the help of the Peruginelli and Bonacci observations (1997). It is worth noting that Kolavani et al. (2019), Bijankhan and Ferro

(2019), and Aniruddha et al. (2020) experimentally observed the effect of different geometrical parameters of a central baffle flume.

Another interesting short-throated flume from a shape perspective is the trapezoidal flume characterized by a V-shaped cross-section, which extends for some distance, and a flat bottom (Robinson and Chamberlain, 1960; Robinson, 1966). A short diverging trapezoidal section ensures the transition between the trapezoidal channel, which is the inlet of the device, and the triangular cross-section channel, as a throat, which is finally followed by a diverging trapezoidal cross-section canal corresponding to the discharge.

In their major study, Ackers and Harrison (1963) gave a full report on the development carried out on trapezoidal flumes at the hydraulics research station of Wallingford. They highlighted foremost that the observation meriting particular attention is that the device calibration curve can be derived, with satisfactory accuracy, from the boundary layer concept involving a drag coefficient. Friction losses within the flume, based on the Darcy-Weisbach friction factor, were determined as a function of the Reynolds number. In addition, design methods were recommended to work out the appropriate flume dimensions for a particular situation.

The operating principle of flumes is based on the transformation of a subcritical flow, evolving in a flat-floored converging section, into a supercritical flow inside a throat, ensuring a "critical transition" between the two in a so-called "control section". The device ends with a diverging part called discharge sections, which is not always necessary, where the flow is subcritical by means of a hydraulic jump or submergence. The operation principle previously described is sometimes based on a localized elevation of the bottom, as seen in the Parshall flume (Bos, 1989; Achour et al., 2003; Achour and Amara, 2023).

Flumes have many advantages over other devices of the same calibre and size, such as weirs. Advantages include the ability to measure high discharges; cause the minimum head loss to vary between 6% and 25% of the head loss caused by a weir, depending on the type of flume, which is a great convenience when the flume is used in areas with low gradients; allow suspended debris to pass more easily, meaning that the device is self-cleaning, unlike the weir, which often requires costly periodic cleaning; and can be built in various sizes. However, some flumes can occupy large spaces and are often based on rectangular cross-sections, whose drawbacks are universally known, such as the low accuracy of flow measurement for shallow flow depths, unlike triangular cross-sections, for which the accuracy is noteworthy even for shallow depths (Achour and Amara, 2022e; Achour and Amara, 2023).

For this reason and because of its simple construction and compactness, requiring less space than the trapezoidal flumes advocated in the past, the present paper intends an in-depth study of a new type of trapezoidal flume, on both theoretical and experimental levels. Hydraulically advantageous, its shape differs from the trapezoidal flumes proposed in previous studies (Robinson and Chamberlain, 1960; Robinson, 1966), generating no flow disturbance along the entire length of the device. Its principle of operation is also based on a lateral contraction of the flow caused by the convergence of

a trapezoidal channel, which accelerates the flow before it pours into a triangular throat, owning a constant apex angle, where a control section originates. The appearance of a control section in the throat is the *sine qua non* condition for the proper operating and performance of the flume as a reliable flow-measuring device. The advocated device does not have a downstream diverging section, although the user can equip it with such a part. In such a configuration, the flume has symmetry with respect to a given vertical axis so that it can be used regardless of the direction of the flow.

Among the features of the device, the ratio of the top width of the throat and the top width of the initial trapezoidal channel cross-section corresponds to the contraction rate of the flume, whose appropriate limit value will be recommended by the authors. This will be derived from an in-depth experimental study conducted on a representative sample of devices. Moreover, based on both geometric and experimental considerations, the optimal device dimensions will be recommended to the designer, especially concerning the appropriate length of the converging trapezoidal canal, the pertinent convergence angle, and the convenient length of the throat.

The advocated flume will be subjected to a theoretical approach that is as rigorous as convincing, with the main objective of deriving the theoretical relationship governing both the discharge coefficient C_d and the flow rate Q. In fact, two theoretical approaches will be recommended to the readers, one based on the energy equation presented in dimensionless terms and the other based on a kinetic factor; both methods, leading to the same result, will rightly account for the effect of the approach flow velocity, which cannot be neglected in the flow measurement field as has often been wrongfully the case in many previous studies.

The study will pursue with laboratory tests carried out in a specially designed hydraulic facility, involving twelve devices of different practical dimensions. Only one device will be presented and developed herein, whose analysis of the resulting observations is the most unfavourable compared to that obtained from the eleven other devices, especially regarding the deviation affecting the discharge coefficient C_d.

Furthermore, the present study plans to either corroborate the derived theoretical relationships, governing C_d and Q, or correct them by the effect of a correction factor resulting from a significant sample of outstanding observations analysis.

MATERIAL AND METHODS

Description of the flume and the resulting flow

Fig. 1 shows a schematic description of the device's plan involving a convergent trapezoidal cross-section channel, of length L_1, extended by a channel of a triangular cross-section of constant opening angle and of length L_2, representing the throat. It is deliberately designated by “DEVICE' “ to define its outline and the space it occupies. It is inserted into a rectangular approach channel whose discharge Q is sought. As shown in Fig. 1, the flume is not connected to the walls of the approach channel by a transition; as

we will see in the appropriate section of the study, this configuration was deliberately chosen so that the cross-sectional shape of the approach channel does not influence the discharge coefficient C_d and hence the discharge Q (Achour and Amara, 2023). Therefore, the flume has the property of being of a universal range, meaning that it can be used regardless of the shape of the approach channel. As seen in Fig. 1a, the flume is equipped with two lateral waterproof vertical plates, placed in section 2-2, each supporting the inclined wall of the throat. In addition to their support role, the waterproof vertical plates act as a barrier preventing water from passing between the walls of the approach channel and the flume, thus creating a water-dead zone that does not participate in the principal flow activity (Fig. 1a). The waterproof vertical plates are anchored in the thickness of each of the walls of the approach channel, and its bottom, via a notch specially designed for this purpose, dug along the half perimeter of section 2-2. Furthermore, there is no elevation either in the bottom of the approach channel or that of the flume, meaning that their longitudinal axes merge, i.e., become one, making the device self-cleaning.

The trapezoidal flume converges from the initial base width b_1 in section 1-1 to the final base width $b_2 = 0$ in section 2-2, where a triangular cross-section is created, whose apex angle is α (Fig. 1b). Angle α is also the constant apex angle of the triangular throat extending the converging trapezoidal channel (Fig. 1b).

Let us define m as the side slope of each side of the converging channel, i.e., m horizontal to 1 vertical. Thus, from Fig. 1b, one may write the following:

$$m = cotg(\theta) = tg\left(\frac{\alpha}{2}\right) \tag{1}$$

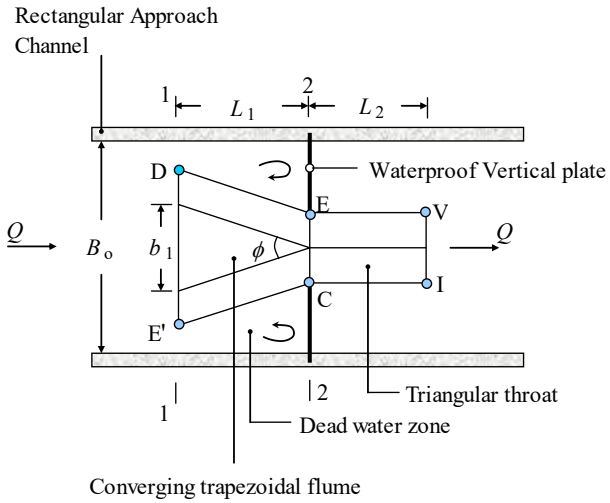

a)

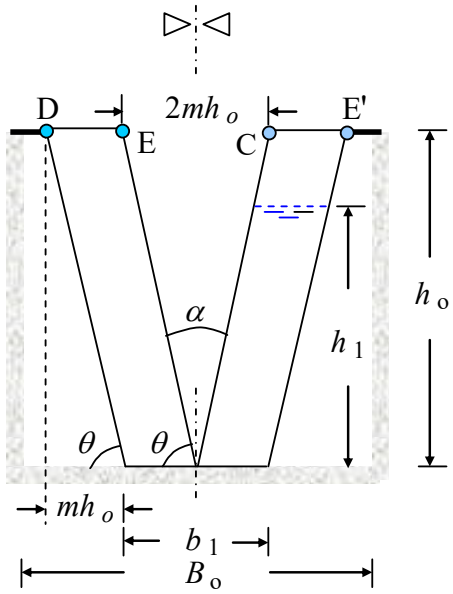

b)

Figure 1: Description of the trapezoidal flume. a) Plan view. b) Front view from upstream

Additionally, according to Fig. 1b, the angles θ and α are related by the following:

$$\theta + \frac{\alpha}{2} = \frac{\pi}{2} \tag{2}$$

Furthermore, as seen in Fig. 1a, angle ϕ corresponds to the angle of convergence whose optimal value is approximately 35°, as the authors' recommendation after analysing intense observations. By adopting this optimal ϕ value, the flow occurs without any disturbance, suitably adhering to the walls of the converging trapezoidal channel. It is important to emphasize that, according to the authors' observations, the value of the angle ϕ must be chosen in the range $30° \leq \varphi \leq 40°$, to create the best flow conditions. Accordingly, one may deduce the following useful optimal result, reasonably rounded, resulting from simple geometric considerations, as: $\frac{L_1}{b_1} \approx 1.60$. Moreover, based on their relevant experimental investigations, the authors recommend adopting a length L_2 for the throat (Fig. 1a) such that $\frac{L_2}{b_1} \approx 2$, i.e.,$L_2 = \frac{5L_1}{4}$.

As shown in Fig. 1a, the considered flume is devoid of a downstream diverging section, as are some flumes, such as the Montana flume (Willeitner et al., 2012). This configuration is the simplest and most economical, especially when the flume works under free flow. Diverging sections are sometimes useful to minimize downstream scour, expand the flow back into the channel, or be the seat of a hydraulic jump. Diverging

sections are not strictly necessary; however, this configuration may be envisaged in the present case, as seen in Fig. 2. As a result, a symmetrical geometric configuration is obtained, with regard to the vertical axis S–S, so that the flume can be used regardless of the direction of the flow, i.e., from left to right or vice versa.

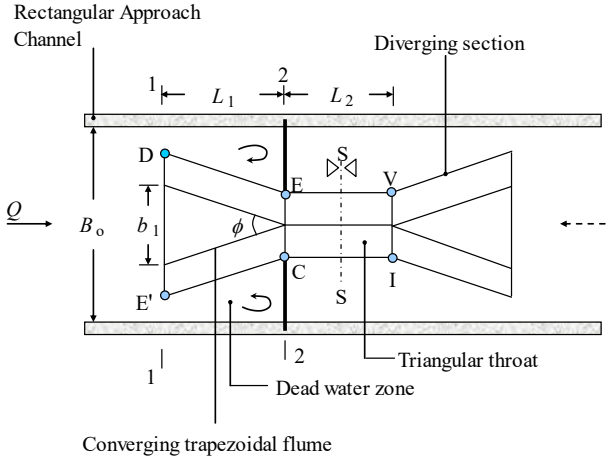

Figure 2: The advocated trapezoidal flume supplied with a diverging section

The flume is inserted into a rectangular approach channel of B_o width and h_o depth (Fig. 1b), whose flow rate Q is sought. The flow depth in section 1-1 (Fig. 1b) is denoted by h_1, and the water cross-sectional area A_1 in this section is defined as:

$$A_1 = b_1 h_1 + m h_1^2 \tag{3}$$

Eq. (3) can be rewritten as follows:

$$A_1 = b_1 h_1 (1 + M_1) \tag{4}$$

Where M_1 is a dimensionless parameter defined as follows:

$$M_1 = \frac{m h_1}{b_1} \tag{5}$$

It can be deduced from Eq. (5) that M_1 can be rewritten as $M_1 = \frac{m h_1^2}{b_1 h_1}$, meaning that M_1 reflects the ratio of the triangular water area of depth h_1 and side slope m to the rectangular water area of width b_1 and of the same depth h_1 (Fig. 1b). It is worth noting that the flume is designed so that $m h_1^2 < (b_1 h_1)$, implying that $M_1 < 1$.

The wetted perimeter in section 1-1 is governed by the following relationship:

$$P_1 = b_1 + 2h_1\sqrt{1 + m^2} \tag{6}$$

According to Fig. 1b, the angle θ can take the maximum value θ_{max} such that:

$$B_o = b_1 + 2 m_{max} h_o \quad (7)$$

Where

$$m_{max} = \text{cotg}(\theta_{max}) \quad (8)$$

Additionally, the horizontal distance $\overline{DE'}$ is such that:

$$\overline{DE'} = b_1 + 2mh_o \quad (9)$$

In section 2-2 (Fig. 2), the horizontal distance $\overline{DE'}$ is reduced to the horizontal distance $\overline{EC}$ as follows:

$$\overline{EC} = 2 m h_o \quad (10)$$

One may define the contraction rate $\beta = \overline{EC}/\overline{DE'}$ (Fig. 2) as $0 < \beta < 1$, which allows us to write the following:

$$\beta = \frac{2 m h_o}{b_1 + 2 m h_o} \quad (11)$$

Eq. (11) can be rewritten as follows:

$$\beta = \left(\frac{1}{2} M_o^{-1} + 1\right)^{-1} \quad (12)$$

Where

$$M_o = \frac{m h_o}{b_1} \quad (13)$$

One may deduce from Eq. (12) the following:

$$M_o = \frac{1}{2}\left(\frac{\beta}{1-\beta}\right) \quad (14)$$

Eq. (14), along with Eq. (13), is mainly intended to calculate the appropriate value of b_1 after having chosen both the contraction β and the value of the side slope m. If the user decides to consider m_{max}, then the appropriate value of b_1 is derived from Eq. (7) for the known value of both B_o and h_o. In addition, Eq. (14) can also be used to calculate the appropriate contraction rate β provided that the initial width b_1 is fixed, bearing in mind that the calculated contraction rate should remain less than or equal to 0.65. Indeed, based on in-depth observations, the authors recommend not exceeding the limit value $\beta = 0.65$; experience shows that values of β less than or equal to 0.65 cause large values of the depth h_1, which is essential for calculating the flow rate Q and allows an accurate depth h_1 reading. Furthermore, choosing the contraction rate β within the range $0 < \beta \leq 0.65$ ensures, in all cases, the appearance of the control section in the throat (Figs. 1 and 3), which is the *sine qua non* condition for the correct operation of the device as a flow

measuring tool. Beyond the limit value $\beta = 0.65$, the depth h_1 would be reduced, inducing an unwanted reading error. In addition, the appearance of the control section in the throat may not be ensured.

Regarding the flow through the flume, the flow depth decreases along the length L_1 due to the effect of the lateral contraction of the flume sides (Fig. 3). The flow remains subcritical along the length L_1, becomes critical in section 2-2 at the entrance of the throat or in a close section further downstream, and then turns into supercritical flow along the length L_2. In Fig. 3, H_1 is the total head in section 1-1, while Hc is the critical total head in section 2-2, at the entrance of the throat, where the subscript c denotes the critical condition.

The critical depth hc in section 2-2 (Fig. 3) is manifested in the triangular section resulting from the gradual lateral contraction of the subcritical flow in the converging trapezoidal channel between sections 1-1 and 2-2.

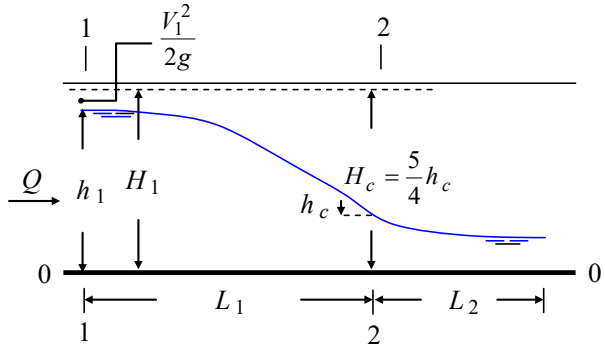

Figure 3: Longitudinal profile of the resulting flow in the advocated trapezoidal flume

The total head H_1 in the initial section 1-1 (Fig. 3) can be expressed as follows:

$$H_1 = h_1 + \frac{Q^2}{2gA_1^2} \tag{15}$$

Inserting Eq. (4) into Eq. (15) results in the following:

$$H_1 = h_1 + \frac{Q^2}{2gb_1^2h_1^2\left(1+M_1\right)^2} \tag{16}$$

Eq. (16) can be rewritten as follows:

$$H_1 = h_1 + \frac{2Q^2}{4gm^2 \frac{b_1^2 h_1^4}{h_1^2 m^2}\left(1+M_1\right)^2} \tag{17}$$

Considering Eq. (5), Eq. (17) becomes the following:

$$H_1 = h_1 + \frac{2Q^2}{4gm^2 \frac{h_1^4}{M_1^2}\left(1+M_1\right)^2} \tag{18}$$

In addition, one may recognize in Eq. (18) the well-known relationship governing the critical depth h_c in a triangular cross-section, such as that occurs in the throat, as follows:

$$h_c^5 = \frac{2Q^2}{gm^2} \tag{19}$$

Inserting Eq. (19) into Eq. (18) and rearranging yields the following:

$$H_1 = h_1\left[1 + \frac{1}{4h_1^{*5}\left(1+M_1^{-1}\right)^2}\right] \tag{20}$$

Where

$$h_1^* = \frac{h_1}{h_c} \tag{21}$$

The flow is subcritical in section 1-1 (Fig. 3), meaning that $h_1 > h_c$; Thus, Eq. (21) indicates that the relative flow depth $h_1^*$is strictly greater than 1.

Eq. (20) can be written in the following simple form:

$$H_1 = h_1(1+\delta) \tag{20a}$$

Where δ, reflecting the effect of the mean approach flow velocity head, is a dimensionless kinetic factor expressed as follows:

$$\delta = \frac{1}{4\,h_1^{*5}\left(1+M_1^{-1}\right)^2} \tag{22}$$

Since h_1^* is greater than 1 and M_1 is less than 1, Eq. (22) indicates that the kinetic factor δ is less than 1. When the kinetic factor δ is close to 0, then the total head H_1 can be equated to the depth h_1 in accordance with Eq. (20a), meaning that the effect of the approach flow velocity is insignificant.

On the other hand, Eq. (20) can be rewritten in dimensionless terms as follows:

$$H_1^* = h_1^* \left[1 + \frac{1}{4\, h_1^{*5} \left(1 + M_1^{-1} \right)^2} \right] \tag{23}$$

Where

$$H_1^* = H_1 / h_c \tag{24}$$

In one of the appropriate sections of the study, the crucial role that both Eqs (22) and (23) play in deriving the sought discharge coefficient C_d of the flume will be highlighted.

Dimensional analysis and discharge coefficient dependency

In this section, dimensional analysis is used to study the general form of the physical equation that governs the discharge coefficient of the flume under consideration. Information will be obtained on the physical phenomenon accounting for only the fact that it must be described by a dimensionally correct equation with respect to influential variables. As a first step, the dimensional analysis requires the counting of these variables and the downgrading their number as much as possible by transforming them into dimensionless parameters.

To enumerate the influential variables, the user often resorts to his intuition. In the present case, one may identify the following influential parameters: the discharge Q, the width b_1, the depth h_1, the apex angle α or the side slope m according to Eq. (1), the acceleration due to gravity g, the density of the flowing liquid ρ, the dynamic viscosity μ of the liquid, and the surface tension σ. The logically discarded parameter is the width B_o of the rectangular approach channel because it is predictable that this variable will not influence the discharge coefficient C_d since there is no transition between the approach channel and the considered flume (Achour and Amara, 2023). The functional relationship that interrelates the variables mentioned above can be written as follows:

$$f(Q, \rho, g, b_1, h_1, \mu, \sigma, m) = 0 \tag{25}$$

The second step required when using dimensional analysis is to always call upon the Vashy-Buckingham π theorem (Langhaar, 1962), along with Eq. (25), to derive the functional relationship that governs the discharge Q as a function of dimensionless parameters. The final result is the following:

$$Q = \sqrt{g}\, m\, h_1^{5/2} \zeta \left(\frac{\rho \sqrt{g}\, {h_1}^{3/2}}{\mu}, \frac{\rho\, g\, {h_1}^2}{\sigma}, \frac{m\, h_1}{b_1} \right) \tag{26}$$

Considering the standard form of the stage-discharge relationship of the triangular weir available in the literature (Bos, 1989; Hager, 1986; Achour and Amara, 2021a), one may deduce from Eq. (26) the following relevant C_d functional relationship:

$$C_d = \psi\left(\frac{m h_1}{b_1}\right) = \psi\left(M_1\right) \tag{27}$$

Thus, the Reynolds number R_e and the Weber number W_e are easily recognized as the first and the second terms in brackets, respectively. Moreover, the effect of the Reynolds number is insignificant in the present case due to the turbulent flow regime prevailing in the current flume. This is also the case for the Weber number because the surface tension only appears for low flow rates, inducing shallow upstream depths, and for small opening angles of the triangular cross-section of the throat. Such conditions are not involved herein, especially during the experimental study. Taking the previous considerations into account along with Eq. (5), Eq. (27) then reduces to the following:

$$C_d = \psi\left(\frac{mh_1}{b_1}\right) = \psi(M_1) \tag{28}$$

Thus, Eq. (28) indicates that the discharge coefficient C_d of the investigated flume depends solely on the dimensionless parameter M_1. The function ψ will be defined in the next section using rigorous theory.

Discharge and discharge coefficient relationships

Using the energy equation

Considering the head loss along the short distance L_1 (Fig. 3) to be negligible, one may write $H_1 = H$c (Fig. 3). Knowing that the flow at the entrance of the throat is critical whose total head is as Hc = 5hc/4, yields the following:

$$H_1 = \frac{5}{4} h_c \tag{29}$$

Taking into account Eq. (24), Eq. (29) reduces to the following:

$$H_1^* = \frac{5}{4} = Constant \tag{30}$$

On the other hand, combining Eqs. (23) and (30) results in the following:

$$h_1^* + \frac{1}{4\, h_1^{*4}\left(1 + M_1^{-1}\right)^2} = \frac{5}{4} \tag{31}$$

Eq. (31) is a quintic equation in h_1^*such that:

$$h_1^{*5} - \frac{5}{4} h_1^{*4} + \frac{1}{4\left(1 + M_1^{-1}\right)^2} = 0 \tag{32}$$

Eq. (32) can be rewritten in the following form:

$$h_1^{*5} - \frac{5}{4} h_1^{*4} + \frac{1}{4}\left(\frac{M_1}{1+M_1}\right)^2 = 0 \tag{33}$$

Thus, one may deduce from Eq. (33) that the relative upstream depth h_1^*depends solely on the dimensionless parameter M_1.

For $M_1 \to 0$, corresponding to $b_1 \to \infty$ in accordance with Eq. (5), Eq. (33) is reduced to the following:

$$h_1^{*5} - \frac{5}{4} h_1^{*4} = 0 \tag{34}$$

With the exception of the trivial solution $h_1^* = 0$, the only root of Eq. (34) to be considered is

$$h_1^* = 5/4 = 1.25 \tag{35}$$

This corresponds to the largest value that h_1^* can reach. Additionally, both Eqs. (30) and (35) yields the following:

$$H_1^* = h_1^* = \frac{5}{4} \tag{36}$$

This configuration corresponds to the case where $H_1 = h_1$, meaning that the effect of the approach flow velocity is insignificant, i.e. $\delta \to 0$.

On the other hand, for $M_1 \to \infty$, corresponding to low values of the initial width b_1 in accordance with Eq. (5), i.e., $b_1 \to 0$, Eq. (32) allows us to write the following:

$$h_1^{*5} - \frac{5}{4} h_1^{*4} + \frac{1}{4} = 0 \tag{37}$$

Eq. (37) is satisfied only for $h_1^* = 1$, meaning that the flow reaches the critical state not only in section 1-1 (Fig. 3), but also along the length L_1.

In the following, what is sought is the determination of h_1^*using Eq. (33) for the known value of M_1. However, Eq. (33) is implicit in $h_1^*$and its resolution is not easy. The best way to solve the problem is to find an accurate explicit approximate relationship. An intense program of calculations has allowed us to deduce that the following explicit relationship is the most appropriate, inspired by Hoerl's model (Kolb, 1982):

$$h_{1,app}^* = 0.24914 - 0.21763\, M_1^{1.09253} + 1.1905^{M_1} \tag{38}$$

Where the subscript "*app*" denotes "Approximate". The approximate Eq. (38) is valid within the wide range $0.10 \le M_1 \le 0.95$, thus encompassing all practical cases. This causes a maximum deviation of less than 0.0012% compared to the exact implicit Eq. (33).

On the other hand, eliminating the critical depth h_c between Eqs. (19) and (21) results in the following discharge Q relationship:

$$Q = \frac{1}{2}\sqrt{2g}\, m\, h_1^{*\,-5/2} h_1^{5/2} \tag{39}$$

The standard form of the stage-discharge relationship governing triangular cross-sections, such as triangular weirs, is as follows (Bos, 1989; Hager, 1986; Achour and Amara, 2021a), highlighting that this relationship also governs the flow rate that passes through the initial section of the throat, similar to a suppressed triangular weir without a crest height:

$$Q = \frac{8}{15} C_d\ m \sqrt{2g}\ h_1^{5/2} \tag{40}$$

Thus, the comparison between both Eqs. (39) and (40) results in the following exact discharge coefficient C_d relationship of the flume, depending solely on the upstream relative depthh_1^* and hence on M_1 according to Eq. (33):

$$C_d = \frac{15}{16} h_1^{*\,-5/2} \tag{41}$$

To calculate the exact value of the discharge coefficient C_d using Eq. (41), the upstream relative depth h_1^* must be derived from Eq. (33) for the known value of the dimensionless parameter M_1. To do so, an iterative procedure must be applied due to the implicit form of Eq. (33). To avoid the drawbacks of such a calculation, it is recommended to use the excellent approximate relationship (38) for the estimation ofh_1^*. Thus, the discharge coefficient C_d of the flume can be calculated according to the following explicit relationship:

$$C_d = \frac{15}{16}\left(0.24914 - 0.21763\, M_1^{1.09253} + 1.1905^{M_1} \right)^{-5/2} \tag{42}$$

Within the validity range $0.10 \le M_1 \le 0.95$, Eq. (42) causes a maximum deviation of less than 0.003% compared to the exact Eq. (41), along with Eq. (33). According to Eq. (41), the above mentioned maximum deviation was predictable since one may write the following:

$$\frac{\Delta C_d}{C_d} = \frac{5}{2}\frac{\Delta h_1^*}{h_1^*} \tag{43}$$

It was previously stated that approximate Eq. (38) causes a maximum deviation of less than 0.0012% in the calculation of the relative depthh_1^*. Thus, according to Eq. (43), the maximum deviation caused on the discharge coefficient C_d computation using approximate Eq. (42) is such that:

$$\frac{\Delta C_d}{C_d} < \frac{5}{2} \times 0.0012 = 0.003\,\% \tag{44}$$

With the known value of M_1 and that of the upstream depth h_1 resulting from the reading gauge, the discharge sought Q is easily computed using Eq. (40), along with Eq. (42), with the same maximum deviation previously indicated, due to the approximation made on the h_1^*calculation.

Fig. 4 shows the distribution of deviations caused by using the approximate Eq. (42) to calculate the discharge coefficient C_d, within the previously indicated validity range of M_1.

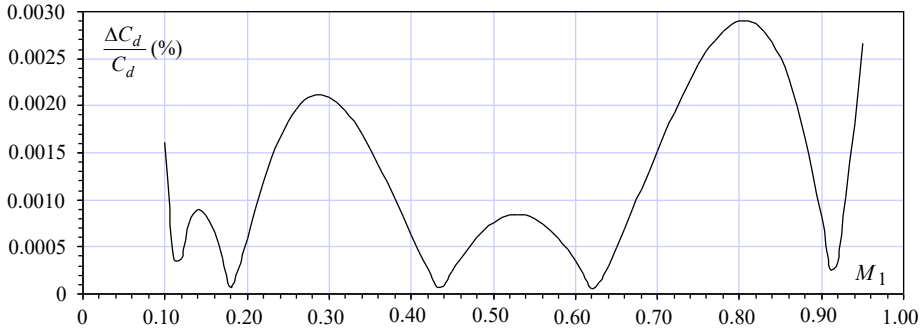

Figure 4: Deviations caused by the approximate Eq. (42) on the calculation of C_d within the validity range of M_1

Fig. 5 shows the variation in the exact discharge coefficient C_d as a function of M_1, according to Eq. (41) along with Eq. (33) solved by an iterative process.

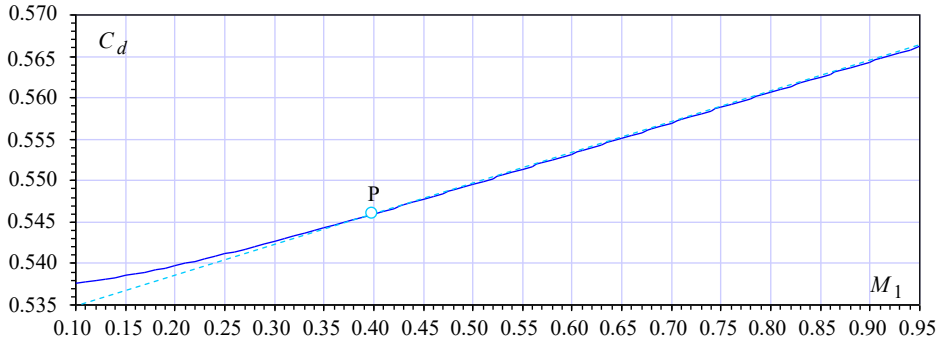

Figure 5: Variation in $C_d(M_1)$ according to Eq. (41) along with Eq. (33)

As can be seen, the discharge coefficient C_d increases with increasing M_1. The most relevant observation is that beyond the point P of coordinates (0.40; 0.546) indicated in Fig. 5, i.e., for values of M_1 such that $M_1 \geq 0.40$, the curve of variation of C_d (M_1) degenerates into a straight line, as indicated by the broken line. A linear fit based on a statistical program showed that this straight line is governed by the following relationship:

$$C_d = 0.0369\ M_1 + 0.5311 \tag{45}$$

Eq. (45) was determined with a coefficient of determination $R^2 = 1$, and the maximum deviation it causes in the calculation of the discharge coefficient C_d is 0.024%, compared to the exact value given by Eq. (41) along with Eq. (33), provided that $M_1 \geq 0.40$.

Using the kinetic factor

Combining Eqs. (19), (29) and (21a) yields the following:

$$\left(\frac{2Q^2}{g\,m^2}\right)^{1/5} = \frac{4}{5}\left(1+\delta\right) h_1 \tag{46}$$

This allows us to write the discharge Q in the following form:

$$Q^2 = \frac{1}{2}\left(\frac{4}{5}\right)^5 m^2 g\left(1+\delta\right)^5 h_1^5 \tag{47}$$

Comparing Eq. (47) with Eq. (40) results in the following:

$$C_d = C_0\left(1+\delta\right)^{5/2} \tag{48}$$

Where C_0 is a constant defined as follows:

$$C_0 = \frac{15}{16}\left(\frac{4}{5}\right)^{5/2} \tag{49}$$

Notably, both Eq. (41), derived from the transformation of the energy equation, and Eq. (48) derived from the kinetic factor-based approach give the same result within the validity range $0.10 \leq M_1 \leq 0.95$. Recall that the kinetic factor δ is governed by Eq. (22) along with exact Eq. (33) or approximate Eq. (38). As the relative depth h_1^* is related to the dimensionless parameter M_1 in accordance with Eq. (33), one may deduce that the kinetic factor δ depends exclusively on M_1. Using Eq. (33) along with Eq. (22), it can be shown that the kinetic factor varies within the following range $0.000679 \leq \delta \leq 0.02164$ for M_1 varying between 0.10 and 0.95. Some might claim that since δ is much less than 1, it can be neglected, meaning that the discharge coefficient of the considered flume is a constant according to Eq. (48). However, this would constitute a fatal error because it is the quantity $(1+\delta)$ that intervenes in Eq. (48) governing the discharge coefficient, which cannot be considered to be very close to 1.

As an example, consider the practical value $M_1 = 0.40$ corresponding to $\delta = 0.0069202$, i.e., $(1+\delta)^{5/2} = 1.017395$. Thus, if δ were to be neglected, then the deviation caused when calculating the discharge coefficient C_d would be approximately 1.74%. Moreover, one may easily work out that the deviation reaches 4% for $M_1 = 0.73$.

The considerations developed in the previous subsections are only theoretical. It is necessary either to corroborate them by laboratory observations or to correct them by the effect of a correction factor resulting from the analysis of these observations. This is what is expected during the experimental validation presented in the next section.

Experimental validation

This part of the study has the main objective of corroborating or correcting the theoretical relationships developed in the previous subsections, in particular approximate theoretical Eq. (42), which governs the discharge coefficient C_d of the advocated flume. Any study carried out on flow measurement should contain such an experimental validation approach.

As we have seen, the influencing dimensionless parameter is M_1, which depends in particular on the upstream depth h_1 to be measured and which is in turn related to the experimental flow rate Q through the stage-discharge relationship (40). Thus, h_1 and Q are so important that they must be measured experimentally using devices of irreproachable precision. That is why Q was estimated from the average between the discharge value read on an ultrasonic flow meter and that of the discharge read on a magnetic flow meter; both devices were carefully calibrated. The absolute error caused by this procedure in the estimation of the flow rate Q was ± 0.1 l/s.

The flow rates were varied within the following wide practical range: 0.45 l/s ≤ Q ≤ 132.2 l/s, involving twelve devices of different practical dimensions, carefully designed in plexiglass. All devices have been tested in the specially designed hydraulic platform depicted in Fig. 6.

The upstream flow depth h_1 was measured using a double-precision Vernier point gauge graduated to 1/10th, causing an absolute error of 0.02 mm in the h_1 depth reading (Achour and Amara, 2022). It is worth noting that the shallowest depth h_1 measured during the tests was approximately 52 mm, which gave the largest deviation in the measurement of h_1 equal to 100 x 0.02/52 = 0.03846%. The range of discharges indicated above corresponded to the following range of the upstream depth $h_1$such that 5.2 cm ≤ h_1 ≤ 49.36 cm.

The dimensionless parameter M_1 was varied within the practical range 0.10 ≤ M_1 ≤ 0.95, scrupulously adopting a variation step of 0.01.

The experimental ranges of discharge and depth h_1 values allowed the significant collection of 1023 measurement points of the pair Q-h_1.

Following are the results of the ninety-nine observations carried out on only one of the twelve tested devices, whose dimensions are indicated in Fig. 6. The quality of the observations carried out on the eleven other tested devices is as excellent as that obtained on the current one. It is worth noting that the results of the observations fulfilled on the device presented herein are the most unfavourable compared to those provided by the eleven other tested devices, particularly concerning the deviation affecting the discharge

coefficient. The complete characteristics of the designed trapezoidal flume, tested in a rectangular approach channel 0.90 m wide and 0.50 m deep, are grouped in Table 1.

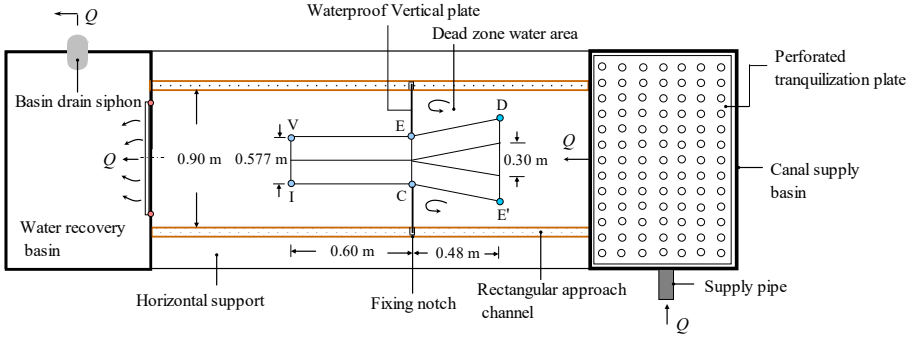

Figure 6: One of the designed devices undergoing testing in the specially designed hydraulic platform

Table 1: Characteristics of one of the tested trapezoidal flumes. Notation according to Figs. 1a and 1b

L_1 (cm)	L_2 (cm)	b_1 (cm)	θ (°)	α (°)	ϕ (°)	h_o (cm)
48	60	30	60	60	35	50

Each of the pairs (Q_{Exp}; $h_{1,Exp}$) collected, where the subscript "*Exp*" denotes "Experimental", allows us to calculate the experimental discharge coefficient $C_{d,Exp}$ of the flume in accordance with Eq. (40), such as:

$$C_{d,Exp} = \frac{15}{8} \frac{Q_{Exp}}{m\sqrt{2g}\, h_{1,Exp}^{5/2}} \tag{40a}$$

Each of the experimental discharge coefficients calculated according to Eq. (40a) was compared with the theoretical discharge coefficient $C_{d,Th}$ computed in conformity with the approximate Eq. (42), for the given experimental value of M_1. The values of $C_{d,Exp}$ and $C_{d,Th}$ are reported in Fig. 7, where the solid curve represents $C_{d,Th}$ and the open signs represent the authors' observations.

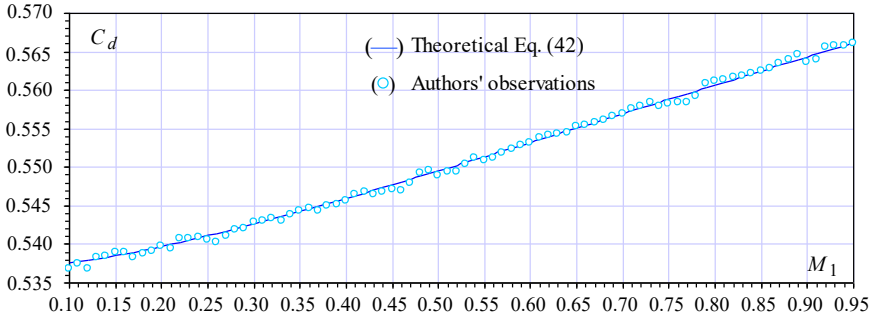

Figure 7: Variation in the predicted and the observed discharge coefficients C_d against M_1 for the tested trapezoidal flume described in Fig. 6

Fig. 7 shows a good agreement between the predicted and observed values, indicating that the model expressed by the approximate Eq. (42) has satisfactory, even excellent, predictive ability. Thus, Eq. (42), governing the discharge coefficient C_d of the advocated trapezoidal flume, requires no correction thereby it can be used in its current form with great assurance and confidence. In addition, compared to observations, Eq. (42) yields 0.215% as a maximum deviation in the calculation of C_d, as reported in Table 2, within the whole range of validity of M_1, i.e., $0.10 \leq M_1 \leq 0.95$. Moreover, the calculation revealed that 95.96% of the deviations are less than 0.20% within the previously mentioned validity range of M_1. Fig. 8 brings out this quality finding.

Table 2: Deviation in the C_d calculation caused by Eq. (42)

Range of M_1	Deviation $\Delta C_d/C_d$(%)induced by using Eq. (42)		
	Minimum	Maximum	Average
[0.10; 0.95]	0	0.215	0.0664

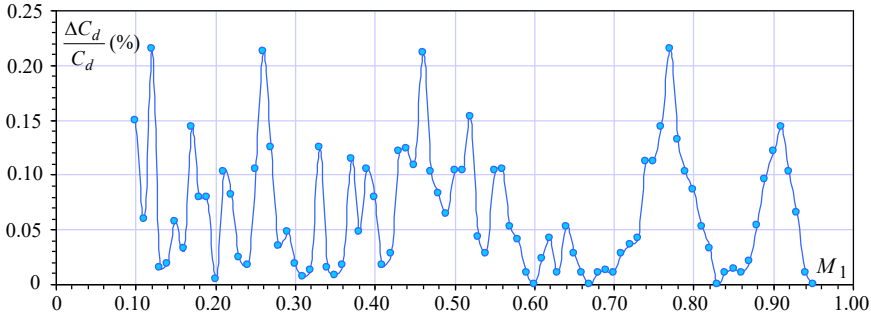

Figure 8: Distribution of deviations induced by Eq. (42) within the validity range $0.10 \leq M_1 \leq 0.95$

CONCLUSION

Each of the twelve investigated trapezoidal flumes is a universal range device intended for accurate flow measurement in open channels regardless of the shape. Its principle of operation is based on the lateral contraction of the flow. Each device is conceived by a converging trapezoidal channel that ends in a triangular throat of constant apex angle. The converging section accelerates the flow from a subcritical state to a critical state in the throat where a control section is created. This is the *sine qua non* condition for the convenient operation of the flume.

The advocated trapezoidal flume differs from other known trapezoidal flumes by its compact shape requiring a minimum of space.

From the point of view of geometry, the contraction rate of the device should not exceed $\beta = 0.65$, according to the tests carried out by the authors, while the optimal convergence angle ϕ should be 35°. These are the optimal parameters that allow the creation of a control section in the throat within the wide range of validity $0.10 \leq M_1 \leq 0.95$, with $M_1 = m h_1/b_1$, where m is the side slope of the trapezoidal converging section, h_1 is the upstream depth measured at the inlet of the converging section, and b_1 is the base width of the initial cross-section of the converging section.

The trapezoidal flume suggested herein lacks a diverging section, which is not required in the proper and convenient operation of flumes. However, if the user is predicting an exposedness probability of downstream scours, thus the diverging section would be useful. In this configuration, the trapezoidal flume has perfect symmetry related to a given vertical axis, proffering the advantage of using the device regardless of the direction of the flow.

In addition, based on intensive experimental investigations, the optimal dimensions of the device have been suggested, including the appropriate throat length, the required length of the converging trapezoidal canal, and the suitable divergence angle. These optimal parameters ensure an undisturbed flow, adhering perfectly to the device walls, as was distinctly observed during laboratory tests.

On the other hand, the study theoretically derived the relationship that governs the discharge coefficient C_d of the flume, using two irreproachably rigorous methods which led to the same result. The first method was based on the transformed energy equation in dimensionless terms, and the second was based on a newly developed kinetic factor. Both methods have rightly accounted for the effect of the approach flow velocity, and the relationship governing the discharge coefficient C_d was then derived. It has been shown that C_d depends solely on M_1, and its variation is linear for $M_1 \geq 0.40$.

Tests carried out in a specially designed hydraulic installation allowed the collection of 1023 measurement points of the pair Q-h_1. Analysis of the collected data revealed with achievement an excellent agreement between the predicted and observed values of C_d, meaning that the derived theoretical discharge coefficient relationship needs no correction. Thus, it can be used in its current form with great assurance and confidence.

Declaration of competing interest

The authors declare that they have no known competing financial interests or personal relationships that could have appeared to influence the work reported in this paper.

REFERENCES

ACHOUR B., AMARA L. (2021a). Discharge coefficient for a triangular notch weir-theory and experimental analysis, Larhyss Journal, No 46, pp. 7-19.

ACHOUR B., AMARA L. (2021b). Theoretical discharge coefficient relationship for contracted and suppressed rectangular weirs, Larhyss Journal, No 45, pp. 165-182.

AMARA L., ACHOUR B. (2021). Theoretical approach to stage-discharge relationship for a circular sharp-crested weir, Technical Note, Larhyss Journal, No 46, pp. 101-113.

ACHOUR B., AMARA L. (2022a). Flow measurement using a triangular broad crested weir-theory and experimental validation, Flow Measurement and Instrumentation, Vol. 83, Paper ID 102088.

ACHOUR B., AMARA L., MEHTA D. (2022b). Control of the hydraulic jump by a thin-crested sill in a rectangular channel, new experimental considerations, Larhyss Journal, No 50, pp. 31-48.

ACHOUR B., AMARA L., MEHTA D., BALAGANESAN P. (2022c). Compactness of Hydraulic Jump Rectangular Stilling Basins Using a Broad-Crested Sill, Larhyss Journal, No 51, pp. 31-41.

ACHOUR B., AMARA L., MEHTA D. (2022d). New theoretical considerations on the gradually varied flow in a triangular channel, Larhyss Journal, No 50, pp. 7-29.

ACHOUR B., AMARA L. (2022e). Triangular broad crested weir, theory and experiment, Larhyss Journal, No 49, pp. 37-66.

ACHOUR B., AMARA L. (2022f). Accurate discharge coefficient relationship for the Crump weir, Larhyss Journal, No 52, pp. 93-115.

ACHOUR B., BOUZIANE T., NEBBAR K. (2003). Triangular broad crested flowmeter in a rectangular channel (Part one), Larhyss Journal, No 2, pp. 7-43 (In French).

ACHOUR B. (1989). Jump flowmeter in a channel of triangular cross-section without weir, Journal of Hydraulic Research, Vol. 27, Issue 2, pp. 205–214 (In French).

ACHOUR B., DE LAPRAY G. (2023). Curved Wall Triangular Flume (CWTF), Design, Theory, and Experiment, Larhyss Journal, No 56, pp. 139-178.

ACHOUR B., AMARA L. (2023). The 2A triangular weir, Design, Theory and Experiment, Larhyss Journal, No 55, pp. 191-213.

ACKERS P., HARRISON A.J.M. (1963). Critical depth flumes for slow measurement in open channels, Hydraulics research paper No 5, Hydraulics Research Station, Wallingford, Berkshire, England.

ANIRUDDHA D.G., ANKUR K., AVINASH B.M. (2020). Cylindrical central baffle flume for flow measurements in open channels, Technical note, Journal of Irrigation and Drainage Engineering, Vol. 146, Issue 9, pp. 1–9.

BIJANKHAN M., FERRO V. (2019). Experimental study on triangular central baffle flume, Flow Measurement and Instrumentation, Vol. 70, Paper ID 101641.

BOS M.G. (1989). Discharge Measurement Structures, third Edition, Publication 20, International Institute for Land Reclamation and Improvement, Wageningen, The Netherlands.

CARLIER M. (1987). General and applied hydraulics, Collection of the Directorate of Studies and Research of "Electricité de France" (EDF), Eyrolles Edtions, Paris, France, 582p. (In French)

FERRO V. (2016). Simple flume with a central baffle, Flow Measurement and Instrumentation, Vol. 52, pp. 53–56.

GOURYEV A.P., BRAKENI A., BEGLAROVA E.C. (2020). Discharge coefficient of shaft spillway under small heads, Larhyss Journal, No 42, pp. 23-39.

HAGER W.H. (1986). Discharge measurement structures, Communication 1, Department of Civil Engineering, the Federal Polytechnic School of Lausanne, Switzerland.

KOLAVANI F.L., BIJANKHAN M., DI STEFANO C., FERRO V., MAZDEH A.M. (2019). Experimental study of central baffle flume, Journal of Irrigation and Drainage Engineering, Vol. 145, Issue 3.

KOLB W.M. (1982). Curve fitting for programmable calculators, Imtec, Maryland, USA.

KULKARNI K.H., HINGE G.A. (2021). Performance enhancement in discharge measurement by compound broad crested weir with additive manufacturing, Larhyss Journal, No 48, pp. 169-188.

KULKARNI K.H., HINGE G.A. (2023). An energy perspective of composite broad crested weir for measuring accurate discharge, Larhyss Journal, No 54, pp. 85-106.

LANGHAAR H.L. (1962). Dimensional Analysis and Theory of Models, Wiley and Sons Inc.

PERUGINELLI A., BONACCI F. (1997). Mobile prisms for flow measurement in rectangular channels, Journal of Irrigation and Drainage Engineering, Vol. 123, Issue 3, pp. 170–174.

REPLOGLE J.A. (1975). Critical flow flumes with complex cross sections, in: Proceeding, Irrigation and Drainage Division, Specialty Conference, ASCE, New York, pp. 336–338.

ROBINSON A.R. (1966). Water Measurement in Small Irrigation Channel Using Trapezoidal Flumes, Transaction ASCE, Vol. 9, Issue 3, Paper 0382–0385.

ROBINSON A.R., CHAMBERLAIN A.R. (1960). Trapezoidal flumes for open-channel flow measurement, Transactions ASAE, Vol. 3, Issue 2, pp. 120-124.

SAMANI Z., JORAT S., YOUSEF M. (1991). Hydraulic characteristics of circular flume, Journal of Irrigation and Drainage Engineering, ASCE, Vol. 117, Issue 4, pp. 558–566.

SAMANI Z., MAGALLANEZ H. (2000). Simple flume for flow measurement in open channel, Journal of Irrigation and Drainage Engineering, ASCE, Vol. 126, Issue 2, pp. 127–129.

SKOGERBOE G.V. BENNETT R.S., WALKER W.R. (1972). Generalized discharge relations for cutthroat flumes, Journal of Irrigation and Drainage Engineering, ASCE Vol. 98, Issue 4, pp. 569–583.

WILLEITNER R.P., BARFUSS S.L., JOHNSON C.M. (2012). Montana flume flow corrections under submerged flow, Journal of Irrigation and Drainage Engineering, ASCE, Vol. 138, Issue 7, pp. 685-689.